Nonlinear polarization interferometer: application for efficient cross polarized wave generation and beam shaping

S. Kourtev[1,*], N. Minkovski[1], O. Albert[2], A. Jullien[2], S.M. Saltiel[1], J. Etchepare[2]
[1]Faculty of Physics, University of Sofia, 5 J. Bourchier Blvd., BG-1164, Sofia, Bulgaria
[2]Laboratoire d'Optique Appliquée, UMR 7639 CNRS, Ecole Polytechnique, ENSTA, 91761 Palaiseau cedex, France

ABSTRACT

Novel $\chi^{(3)}$-based nonlinear polarization interferometer is proposed. It allows cross polarized wave generation with enhanced efficiency and obtaining different beam shapes of the generated cross-polarized wave. The interferometer consists of two polarizers, two quarter-wave plates and a BaF_2 crystal. The experiment with this interferometer confirms the predicted dependences.

Keywords: Polarization interferometer, Cross-polarized wave generation, Beam shaping

1. INTRODUCTION

Frequency conversion is one of the main areas of application of nonlinear optical devices. Another field of application is controllable modification of laser parameters. With the means of nonlinear optics one can induce chirp, do compression or stretching, change the polarization properties of the laser radiation, deflect the beam and etc. In this direction we recently demonstrated that with the $\chi^{(3)}$-based cross-polarized wave (XPW) generation device the temporal contrast of femtosecond pulses can be greatly improved[1]. Here we propose a modification of the XPW generation device proposing on its base nonlinear polarization interferometer (NPI). We demonstrate both theoretically and in the experiment enhanced efficiency of the XPW generation and possibility to use this device to obtain different spatial shapes of the generated XPW beam. Beam shaping is very important in a number of applications[2].

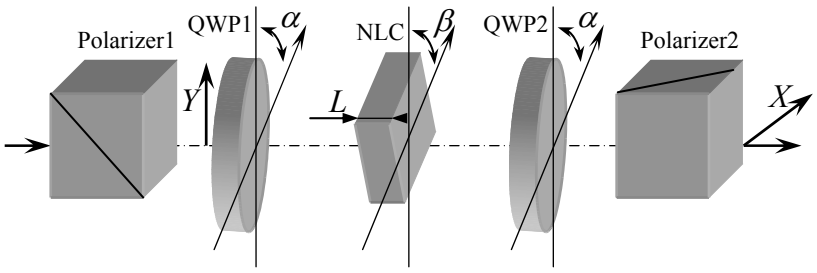

Fig. 1. Scheme of the XPW-based nonlinear polarization interferometer.

The nonlinear polarization interferometer is shown on Fig. 1. It consists of a sandwiched structure made of a non linear cubic crystal (NLC) placed between two identical quarter wave plates (QWP1 and QWP2). The sandwiched structure is located between two crossed polarizer. This device, shown in Fig. 1, corresponds to an unfolded version of the nonlinear mirror[3] previously investigated with the aim to demonstrate intensity dependent reflection. The genuine version that did not use any quarter-wave plate, enabled generation of a cross polarized wave and has been successfully used for improving femtosecond pulse contrast ratio[1]. Another XPW generation device with two QWPs has been investigated in Ref. 4 where the second QWP is crossed to the first one i.e. at angle $\pi/2+\alpha$. For the device we investigate here the second QWP is not crossed and is turned at the same angle as the first one. This has dramatic impact on the performance and this is the reason we investigate this version in details.

* skourtev@phys.uni-sofia.bg

14th International School on Quantum Electronics: Laser Physics and Applications,
edited by Peter A. Atanasov, Tanja N. Dreischuh, Sanka V. Gateva, Lubomir M. Kovachev,
Proc. of SPIE Vol. 6604, 66041E, (2007) 0277-786X/07/$15 doi: 10.1117/12.726983

The device shown on Fig. 1 uses the Mach-Zehnder interferometer principle. The first quarter wave plate QWP1 that is rotated by a relatively small angle splits the linear polarized wave into two orthogonally polarized waves (pump and probe) with $\pi/2$ relative phase shift. In the nonlinear crystal the pump produces by $\chi^{(3)}$-effect a XPW that is also shifted by $\pi/2$ with respect to the pump. The two waves, the probe and the generated XPW, interfere modifying the amplitude of the probe beam. After the second quarter-wave plate QWP2 pump and probe waves transform into a single linear polarized wave that comes out after Polarizer2 as a wave with polarization perpendicular to the input one. We predict that the output XPW beam compared to the input beam can have a different spatial shape depending on the input intensity. We predict also increased efficiency of XPW generation compared with the scheme without quarter wave plates. To demonstrate this let first consider simple analytical model that is valid at relatively low intensity when depletion of the fundamental wave in the nonlinear crystal can be neglected.

2. THEORETICAL MODEL

2.1. Analytical approach in non-depleted regime

After the QWP1 rotated at angle α there are two waves with amplitudes at the input of the nonlinear crystal equal to: $A_0(r,t) = D_0(r,t)\cos\alpha$ (along the fast axis of the QWP1) and $B_0(r,t) = -iD_0(r,t)\sin\alpha$ (along the slow axis of the QWP1). The wave $B_0(r,t)$ is delayed by $\pi/2$ with respect to the wave $A_0(r,t)$ that we will call fundamental. The strong wave $A_0(r,t)$ causes generation of XPW $B(r,t,L)$ in the nonlinear crystal

$$B(r,t,L) = -i\gamma_\perp L\left|D_0(r,t)\right|^2 D_0(r,t)\cos^3\alpha\,, \tag{1}$$

where $\gamma_\perp = -\gamma_0(\sigma/4)\sin 4\beta$, $\gamma_0 = (6\pi/8\lambda n)\chi^{(3)}_{xxxx}$, and $\sigma = \left(\chi^{(3)}_{xxxx} - 2\chi^{(3)}_{xyyx} - \chi^{(3)}_{xxyy}\right)\Big/\chi^{(3)}_{xxxx}$. The two waves $B(r,t,L)$ and $B_0(r,t)$ are in phase and they can interfere constructively or destructively depending on the sign of the product $\gamma_\perp\sin\alpha$. Resulted XPW $E(r,t,L)$ is

$$E(r,t,L) = -i\left[\gamma_\perp L\left|D_0(r,t)\right|^2\cos^3\alpha + D_0(r,t)\sin\alpha\right]. \tag{2}$$

After the second quarter wave plate QWP2. The two wave $E(r,t,L)$ and $A_0(r,t)$ will be in phase and will interfere on polarization plane of the output polarizer. Then the output field will be $C = -A_0(r,t)\sin\alpha - iE(r,t,L)\cos\alpha$. The output intensity will be proportional to

$$\left|C\right|^2 = \left|D_0(r,t)\right|^2\left|\sin 2\alpha + \gamma_\perp L\left|D_0(r,t)\right|^2\cos^4\alpha\right|^2. \tag{3}$$

For XPW generator $\alpha = 0$ the intensity will be

$$\left|C_0\right|^2 = \left[\gamma_\perp L\left|D_0(r,t)\right|^3\right]^2. \tag{4}$$

For finding the energy we integrate (3) and (4) over r and t assuming Gaussian spatial and temporal shape $\left|D_0(r,t)\right|^2 = I_0\exp\left(-2r^2 - 2t^2\right)$. Then the efficiency of XPW generation with NPI will be

$$\eta_{\mathrm{NPI}} = \frac{1}{9}\cos^2\alpha\left[S_\perp^2\sqrt{3}\cos^6\alpha + 9S_\perp\sqrt{2}\cos^3\alpha\sin\alpha + 36\sin^2\alpha\right]. \tag{5}$$

This energy efficiency has to be compared to the energy efficiency of the standard XPW generator

$$\eta_0 = \sqrt{3}S_\perp^2/9\,, \tag{6}$$

where $S_\perp = \gamma_\perp I_0 L$ ($S_\perp = S(\sigma/4)\sin 4\beta$; $S = \gamma_0 I_0 L$; I_0 is the intensity of the input beam at $r = 0$ and $t = 0$. Assuming $\sigma = -1.2$ for BaF_2[5,6] we have $S_\perp = 0.3S$ for $\beta = -\pi/8$.

The comparison of the efficiency of the NPI and the standard XPW generator (dashed curve) according this analytical model (Eqs. 5-6) is shown on Fig. 2a for angles $\alpha = 6°$ and $\alpha = -6°$. Important role plays the sign of the product $S_\perp \sin\alpha$. When it is positive the XPW efficiency is increased and when $S_\perp \sin\alpha < 0$ the efficiency has minimum point which was explored in Ref. 3 for obtaining intensity dependent reflection. The branch A (solid curve on Fig. 2a) corresponds to $S_\perp \sin\alpha > 0$ and branch B (dotted curve) corresponds to $S_\perp \sin\alpha < 0$. In this communication we will investigate the branch B for obtaining different spatial shapes of XPW beam and branch A to demonstrate increased XPW efficiency.

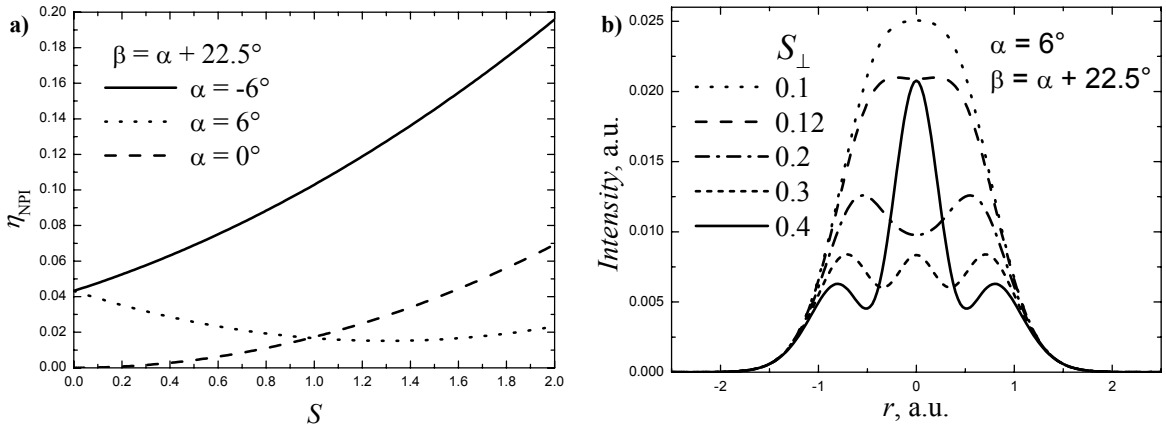

Fig. 2. a) efficiency of the NPI (see Eqns.5 and 6) and **b)** beam profiles (see Eqn.7), obtained using the analytical model.

To demonstrate beam shaping that is result of the interference of the probe wave and the generated XPW wave we perform temporal integration of (3).Then the shape of the generated XPW is

$$B_{\mathrm{XPW}}(r) = \sqrt{\frac{\pi}{6}}\, \mathrm{e}^{-2r^2}\left(S_\perp^2\, \mathrm{e}^{-4r^2}\cos^8\alpha + S_\perp\sqrt{6}\,\mathrm{e}^{-2r^2}\cos^4\alpha\,\sin 2\alpha + \sqrt{3}\sin^2 2\alpha\right). \tag{7}$$

The shapes for $\alpha = 6°$ and different values of the parameter $S_\perp$ are shown on Fig. 2b. It is seen that different types of spatial shapes can be obtained with this NPI.

2.2. Numerical solution

The analytical model allows fast estimation of the behavior of the NPI. At high input intensity when the depletion of the fundamental beam has to be taken into account it is not possible analytical solutions to be obtained and numerical solution of the differential equations describing the process of XPW generation followed by numerical integration of the obtained spatial and temporal shape of the XPW is needed. Other types of spatial and temporal shapes also not always allow analytical solution even within non-depleted regime. The differential equations that describe the XPW generation have been published in Ref. 4. In the experiment hat-top beam was focused with a lens (see Fig. 4) so the spatial shape of the input beam incident on the NLC was approximated in the numerical simulation with radial amplitude distribution of the form $J_1(r)/r$ where $J_1(r)$ is the first order Bessel function of first kind. The temporal shape used in the simulation was secant hyperbolic. The dependence of the efficiency obtained as a result of this numerical approach is shown on Fig. 3a. On Fig. 3b we show several spatial shapes obtained with the same approach.

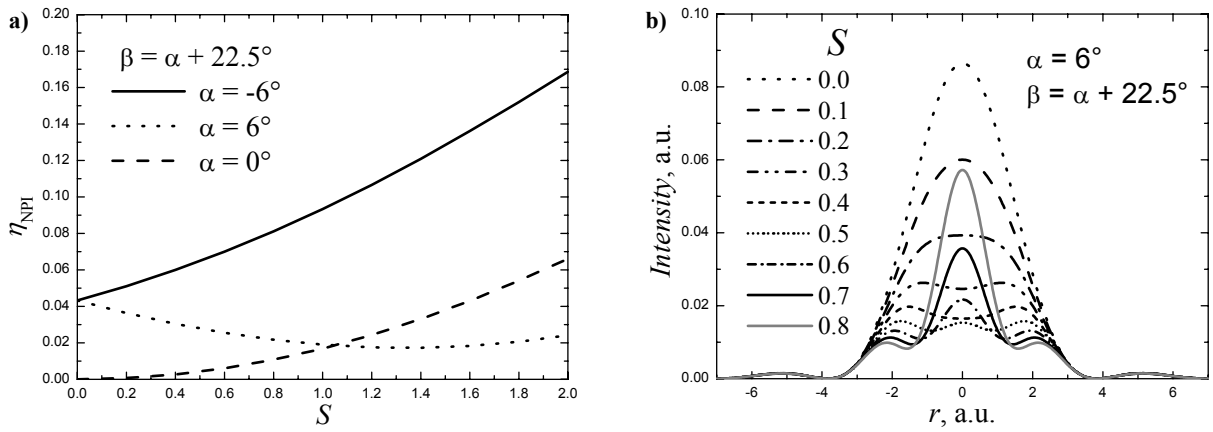

Fig. 3. a) NPI efficiency and **b)** beam shapes, obtained using the numerical approach.

3. EXPERIMENTS AND DISCUSSIONS

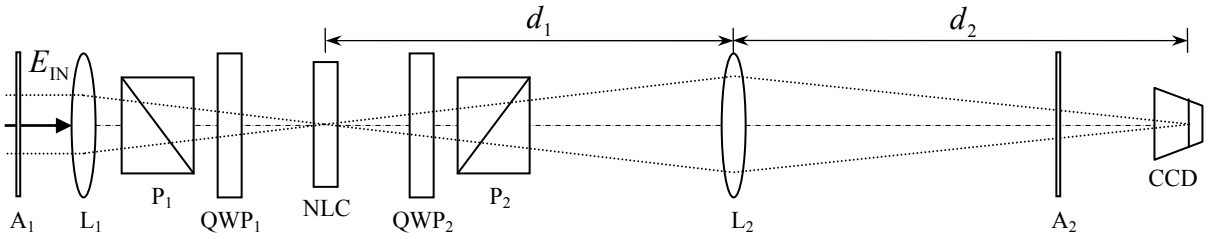

Fig. 4. Experimental setup. A_1, A_2 – attenuation filters; L_1, L_2 – lenses; P_1, P_2 – Glan polarizers; QWP_1, QWP_2 – quarter-wave plates; NLC – BaF_2 crystal; E_{IN} – energy of the input pulses.

Experimental setup is shown in Fig. 4. A_1 and A_2 are neutral-density filters. A_1 was used to tune the input energy E_{IN} while A_2 allows adjusting the intensity of the beam within the dynamic range of the CCD-camera. The NLC was a 2-mm thick *z*-cut BaF_2 crystal placed in the focus of the L_1 lens ($f = 30\,\text{cm}$). The lens L_2 with $f = 50\,\text{cm}$ was used to image and magnify d_2/d_1 -times the spot of the beam emerging from the BaF_2-crystal onto the CCD sensing area. In the experiment L_2 and CCD were placed in such a way that $d_1 = 54.5\,\text{cm}$ and $d_2 = 528\,\text{cm}$ so the beam spot was magnified 9.7 times in the plane of the CCD. A "Hitachi" KP-M1EK CCD-camera with pixel pitch 11 μm x 11 μm was used to record the beam profile. There was no focusing optics mounted on the camera. The polarizers, the lenses, and the NLC were uncoated.

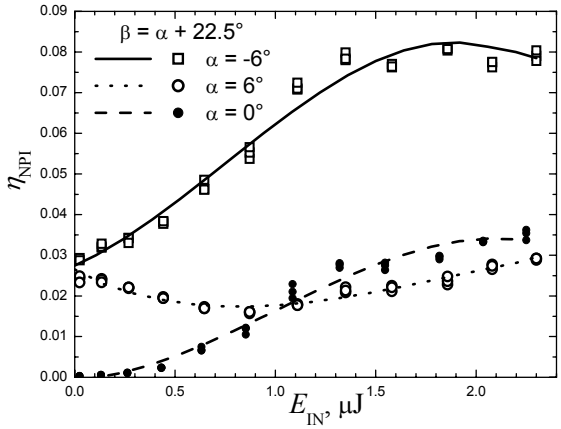

Fig. 5. Experimental dependence of the NPI efficiency on the input energy.

The laser source was a CPM dye-laser with wavelength 620 nm, pulse duration 100 fs, and repetition rate 10 Hz. In all experiments the maximum input energy was less than 5 μJ. For absolute energy measurements an "OPHIR" energy meter was used. Measured conversion efficiency is shown in Fig. 5. Values shown on the figure are not corrected for the reflection losses at uncoated surfaces. As can be seen measured efficiencies are in good qualitative agreement with the theoretical predictions (see Figs. 2a and 3a). Beam shaping

(reshaping) properties were also investigated. Some beam profiles obtained at different input energies are shown in Fig. 6. The experiments that we carried out with the proposed nonlinear polarization interferometer confirmed our theoretically predicted behavior of this device.

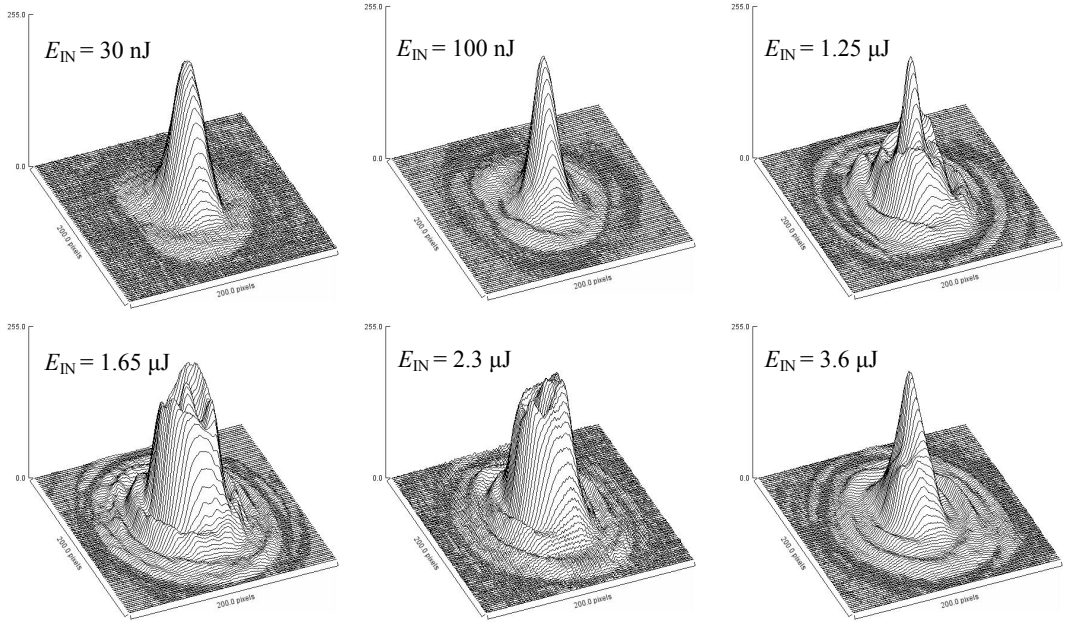

Fig. 6. Experimentally obtained beam profiles at different input energies. Quarter-wave plates were at $\alpha = 6^{\circ}$ and NLC was at $\beta = \alpha + 22.5^{\circ}$.

Due to the enhanced conversion efficiency the proposed nonlinear polarization interferometer can be used for contrast improvement of ultrashort optical pulses instead of the standard XPW-generator when high efficiency and not the contrast ratio is of prime importance. Potential applications of the beam-shaping capability of this device are: micro-machining, laser ablation, medical applications, optical data processing, optical tweezers, etc.

This work was performed within the program "Access to Research Infrastructure" (LaserLab-Europe, R||3-CT-2003-506350). We acknowledge the support by the Bulgarian Science Fund through grant No. 1201/2002.

REFERENCES

1. A. Jullien, O. Albert, F. Burgy, G. Hamoniaux, J.-P. Rousseau, J. –P. Chambaret, F. Augé-Rochereau, G. Chériaux, J. Etchepare, N. Minkovski, and S. M. Saltiel, "10^{-10} temporal contrast for femtosecond ultraintense lasers by cross-polarized wave generation," Opt. Lett. **30**, 920-922 (2005).
2. F. M. Dickey and S. C. Holswade, Eds., *Laser beam shaping. Theory and techniques*, Marcel Dekker, Inc., New York, 2000.
3. S. Kourtev, N. Minkovski, S.M. Saltiel, A. Jullien, O. Albert, and J. Etchepare, "Nonlinear mirror based on cross polarized wave generation," Opt. Lett. **31**, No.21 (11/01/2006).
4. A. Jullien, O. Albert, G. Chériaux, J. Etchepare, S. Kourtev, N. Minkovski, and S. M. Saltiel, "Nonlinear polarization rotation of elliptical light in cubic crystals, with application to cross-polarized wave generation," J. Opt. Soc. Am. B **22**, 2635-2641 (2005).
5. R. DeSalvo, M. Sheik-Bahae, A. A. Said, D. J. Hagan, and E. W. Van Stryland, "Z-scan measurements of the anisotropy of nonlinear refraction and absorption in crystals," Opt. Lett. **18**, 194-196 (1993).
6. N. Minkovski, G. I. Petrov, S. M. Saltiel, O. Albert, and J. Etchepare, "Nonlinear polarization rotation and orthogonal polarization generation experienced in a single-beam configuration," J. Opt. Soc. Am. B **21**, 1659-1664 (2004).